Synchrotron based mass spectrometry to investigate the molecular properties of mineral-organic associations

Suet Yi Liu,[1] Markus Kleber,[2] Lynelle K. Takahashi,[1] Peter Nico,[3] Marco Keiluweit,[2,4] Musahid Ahmed[1,]*

[1] Chemical Science Division, Lawrence Berkeley National Laboratory, Berkeley, CA, USA

[2] Department of Crop and Soil Science, Oregon State University, Corvallis, OR, USA

[3] Earth Sciences Division, Lawrence Berkeley National Laboratory, Berkeley, CA, USA

[4] Chemical Sciences Division, Lawrence Livermore National Laboratory, Livermore, CA, USA.

KEYWORDS

soil organic matter, laser desorption, synchrotron radiation, secondary ion mass spectrometry, tunable VUV.

* Corresponding author, mahmed@lbl.gov

ABSTRACT

Soil organic matter (OM) is important because its decay drives life processes in the biosphere. Analysis of organic compounds in geological systems is difficult because of their intimate association with mineral surfaces. To date there is no procedure capable of quantitatively separating organic from mineral phases without creating artifacts or mass loss. Therefore, analytical techniques that can (a) generate information about both organic and mineral phases simultaneously and (b) allow the examination of predetermined high-interest regions of the sample as opposed to conventional bulk analytical techniques are valuable. Laser Desorption Synchrotron Postionization (synchrotron-LDPI) mass spectrometry is introduced as a novel analytical tool to characterize the molecular properties of organic compounds in mineral-organic samples from terrestrial systems, and it is demonstrated that when combined with Secondary Ion Mass Spectrometry (SIMS), can provide complementary information on mineral composition. Mass spectrometry along a decomposition gradient in density fractions, verifies the consistency of our results with bulk analytical techniques. We further demonstrate that by changing laser and photoionization energies, variations in molecular stability of organic compounds associated with mineral surfaces can be determined. The combination of synchrotron-LDPI and SIMS shows that the energetic conditions involved in desorption and ionization of organic matter may be a greater determinant of mass spectral signatures than the inherent molecular structure of the organic compounds investigated. The latter has implications for molecular models of natural organic matter that are based on mass spectrometric information.

INTRODUCTION

As organic matter decays in soils, it is converted to CO_2 which contributes to the retention of heat in the atmosphere. This process needs to be mechanistically understood in order to avoid carbon-climate feedbacks that may reduce the habitability of the biosphere for humans. Understanding the mechanisms of organic matter transformations requires observations and analyses of organic compounds in geological systems that are difficult for several reasons: (i) soil organic matter is a highly heterogeneous mix of molecularly diverse compounds, (ii) the molecular composition of as much as 50% of these compounds are unknown with (iii) significant contributions of thermally altered materials and finally but probably most significantly for analytical considerations, (iv) mineral phases may interfere with the outcome of conventional analytical procedures. For example, paramagnetic iron can render closely associated carbon atoms invisible to ^{13}C-NMR spectroscopy.[1] Separation of organic matter from mineral phases has often been attempted in soil science and biogeochemistry research, but artifact free and quantitative isolation of organic matter from mineral phases has never been conclusively demonstrated.[2] In addition, mineral-organic interactions have turned out to be meaningful for the persistence of OM in soils[3] suggesting that mechanistic insights can only be gained when organic matter is observed and investigated while in contact with adsorbing, absorbing, entrapping or even catalyzing mineral matrix.

Mass spectrometric (MS) techniques have been used for the characterization of organic matter from natural environments for several decades.[4] A large literature reports data from Pyrolysis-MS, where thermal energy is used to cleave large molecules at their weakest points to produce smaller, more volatile fragments[5] (Pyrolysis is defined as the thermochemical decomposition of organic material at elevated temperatures in the absence of oxygen). These fragments can be

separated by a chromatographic approach (Py-GC-MS)[6,7] or by an electromagnetic field after an ionization step (Field ionization, FI) allows them to become accelerated towards a detector (Py-FI-MS).[8,9] The resulting spectrometric data can either be used as fingerprints to identify materials[10] or allow for a mass based identification of individual fragments to obtain structural information of the parent material.[11] An obvious drawback of pyrolysis-based methods is the risk of thermal artifacts, i.e. the production of thermally modified fragments that were not part of the original parent material.[12] It follows that an analytical capability would be desirable that achieves desorption of chemically complex organic materials from the mineral phase that avoids chemical modifications of the desorbed molecules other than plain fragmentation. The same principle applies to the separation of desorbed compounds for detection; this should also be accomplished without chemical modifications other than fragmentation.

The goal of the research reported in this manuscript is to examine the applicability of a novel mass spectrometric approach to the characterization of mineral-organic associations. Laser Desorption Synchrotron Postionization (synchrotron-LDPI) mass spectrometry has recently been developed to provide a soft desorption method to release molecules on surfaces with minimal input of internal energy and sample damage.[13] Tunable synchrotron Vacuum Ultraviolet Radiation (VUV) has been demonstrated to yield fragment-free mass spectra for fragile organic molecules.[14] This soft ionization method is valuable for the analysis of chemical mixtures by promoting parent ion detection and minimizing the complexity of the resulting mass spectrum.[15,16] The threshold at which radiation provides sufficient energy to produce ionization depends on the composition, molecular structure and phase of the medium. Fixed energy 10.5 electron volts (eV) VUV radiation is often used in mass spectrometry since this is readily available by generating higher harmonics from a commercial laser.[17] However, by changing the

energy of a synchrotron photon beam in small steps, photoionization efficiency (PIE) curves can be obtained for desorbed surface molecular species, allowing the procedure to be tuned for minimum damage to the analyte and to extract information to distinguish different classes of organic matter. We also explored the extent to which corresponding information about the mineral phase could be obtained by combining the synchrotron-LDPI technique with secondary ion mass spectrometry (SIMS), an analytical technique suitable for the investigation of mineral surface properties.

Our conceptual approach towards reaching an assessment of the suitability of the combined synchrotron-LDPI \ SIMS approach for the characterization of mineral-organic associations was to take advantage of the availability of a set of chemically well characterized physical soil fractions.[18] The procedure chosen to isolate these fractions from whole soil has been shown to generate ecologically relevant soil subunits,[19] where relatively undecomposed plant and animal residues (such as lignin and phenolic components) are concentrated in fractions with low density. With increasing density, fractions become progressively enriched with microbial derived decomposition products of significantly different chemistry. This series of soil fractions has been previously characterized[18] with a harsh bulk chemical technique based on alkaline cupric-oxide (CuO) oxidation to quantify lignin[20] as well as cutin- and suberin-derived hydroxyl- and alkoxy-substituted fatty acids (SFA).[21] The availability of those samples together with information on general organic characteristics provided us with a knowledge base against which we could test the plausibility of the combined synchrotron-LDPI \ SIMS approach and its ability to provide better resolved and more specific information about the molecular properties of organic matter in close contact with mineral surfaces.

EXPERIMENTAL SECTION

The experiments were performed on a modified commercial reflectron-type time-of-flight secondary ion mass spectrometer (TOF.SIMS V; IonTOF, Germany) coupled to a synchrotron VUV light port. This apparatus is also equipped with a laser allowing laser desorption followed by VUV synchrotron ionization mass spectrometry. The experimental apparatus and the optical delivery system of the UV laser have been reported elsewhere.[13,22] A 349 nm Nd:YLF desorption laser emitting 8.5 ns pulses is focused to a spot diameter of ~30 μm and irradiates the sample surface at an angle of 45 degrees. Depending on the sample type and analysis desired, various laser peak power densities ranging from ~0.7 MW cm^{-2} to 20 MW cm^{-2} were used. To optimize the signal to noise (S/N) ratio, each data set presented here is the sum of mass spectra collected for ≈ 16000 laser shots on the sample surface. To avoid pyrolysis from laser heating and sample damage, mass spectra are typically collected while the sample is linearly scanned by rastering the sample stage at a fixed speed of 2 mm/sec over a 20 mm distance. A neutral molecular plume desorbed by the laser pulse starts to spread perpendicular to the sample surface, and is intersected by the synchrotron VUV beam, which is approximately 50 μm to 150 μm above the sample surface. Samples are held at ground potential, 1.5 mm away from the analyzer extraction cone of the mass spectrometer. The molecules, after being ionized by the VUV light, continue unaltered in their velocity till application of an extraction electrical field pulse. A 3 μs-long -2kV extraction pulse is applied 2 μs after the desorption laser shot. This delay is used to accumulate more ions in the interaction region and eventually obtain a mass spectrum with a better signal to noise ratio. The spectral width of the ionizing VUV light is ~0.2 eV and when necessary, flux-limiting slits are employed to reduce the photon flux to avoid detector saturation. For the SIMS mass spectra, mass-selected Bi_3^+ ions with 25 keV kinetic energy impact the sample surface at

45°, ejecting cationic, anionic, and neutral chemical species. SIMS spectra are acquired with a 12.5 ns Bi_3^+ pulse over an area of 150 µm × 150 µm, with a 64 pixel × 64 pixel raster scan at a repetition rate of 6.7 kHz (cycle time 150 µs), and secondary ions are extracted with a 10 µs-long, -2 kV pulse.

The density fractions examined in this study originated from a highly weathered Oxisol in Puerto Rico and was obtained by floatation on sodium polytungstate, aspiration of the floating material and supernatant, and vacuum filtration. The characteristics of this soil have been described elsewhere.[18] Originally, the Susua soil was separated into eight different densities (1.60, 1.75, 1.95, 2.15, 2.45, 2.65, 2.80 and 3.00 g cm^{-3}). The samples with densities of 1.75 g cm^{-3} and 1.95 g cm^{-3} were exhausted and not available for this study, hence only the remaining six density fractions and the bulk sample were used in this study.

Samples analyzed by synchrotron-LDPI and SIMS are prepared on silicon substrates (Wafer World, Inc.; P/N 1183) by directly depositing the soil sample (about 5 mg) onto the silicon and subsequently dissolving and dispersing the applied compound with high-purity (99.9%) methanol. Samples are allowed to air-dry.

RESULTS AND DISCUSSION

For complex mixtures of organic compounds, “hard” ionization (i.e. electron impact) is not a preferable technique because the analytes are heavily fragmented, and the overlapping complex fragment patterns cannot be deconvoluted into the mass spectra of individual compounds. Taking advantage of tunable VUV radiation, the analyzed molecules can be ionized at the energies just above their threshold ionization energy, and therefore the fragmentation can be controlled by varying this photon energy. Another factor that can affect the fragmentation process is the power

of the laser. Since the laser-desorption process in which a laser pulse is absorbed by a substrate, converts to heat, and causes thermal desorption, sample molecules would decompose or pyrolyze if intense laser pulses are applied. In this study, we aimed to desorb neutral molecules with less fragmentation, hence all samples were examined at various laser peak power densities and the optimum threshold laser power that was high enough to desorb molecules from a surface but not pyrolyze the sample was determined. The value of this threshold laser power depends on the sample type. In our case, all soil samples had similar threshold laser power of 3.7 MW cm^{-2} (0.22 µJ $pulse^{-1}$).

After the threshold laser power was determined, mass spectra for all density fraction soil samples were collected at different photon energies from 8 eV to 14 eV in 1 eV intervals. Figure 1 a–c shows select spectra of the lightest fraction (LF, 1.6 g cm^{-3}) of the Susua soil at different photon energies. The quality and sensitivity of synchrotron-LDPI is demonstrated by the fact that each spectrum was acquired within ~10 sec which results from the high repetition rate of the 2.5 kHz UV laser used in this study. At 9 eV (figure 1a), there are discrete signal peaks in the high mass region between mass-to-charge ratios (m/z) of 200–500. As the photon energy increases to 14 eV, the fragments at m/z = 149 and below became more prominent, which is thought to arise from dissociative photoionization of neutral molecules (excess energy deposited into the ion which leads to dissociation) (see Fig. 1 b–c). In order to reduce the complexity of the peak assignment, the mass spectra measured at 9 eV were used for mass peak assignment due to less fragmentation and reasonable signal to noise ratio. Since tandem mass spectrometry or ultrahigh-mass-resolution MS detection is not available in our experimental suite at present, the assignment of mass peaks requires some prior chemical knowledge of the investigated system.

It is well known that the primary source for organic matter formation in soil is plant and microbial biomass. Sollins *et al*. reported that the lightest fraction included both lignin and plant-liked fatty acids and a small amount of mineral compounds.[18] synchrotron-LDPI is not sensitive to metals and it is unlikely that mineral compounds appeared with signals in this high mass range (m/z = 200 to 500), therefore, only the contribution of plants and microbes would be considered here. Since aromatics (lignin) and long carbon chains (fatty acid) belong to different classes of organics, it is possible to distinguish them by ionization energy. Photoionization efficiency (PIE) curves for each mass peak observed in the lightest density fraction (1.6 g cm^{-3}) were obtained by varying UV photon energy between 7.4 and 11.0 eV, and mass spectra were collected at 0.1 eV photon energy intervals (see supplementary Fig. S1). The measured ionization energies (IEs) for mass peaks at m/z = 484, 396, 379, 341, 299 were around 7.7 eV, which is similar to the IEs of lignin monomer.[22] The measured IEs for mass peaks at m/z = 284, 256 were around 8.4 eV. Mysak *et al*.[23] measured the IE of three fatty acid samples with similar molecular weight around 280 Da, to be around 8.5 eV. Therefore, it is likely that m/z = 284 and 256 can be attributed to long-chain fatty acids or aliphatic compounds.[17,23] It is also possible that m/z = 284 and 256 could be attributed to the dissociative photoionization of higher masses. However, these two peaks appeared at lower desorption laser energies compared to the mass peaks between m/z = 290–500 (see supplementary Fig. S2). This implies that these peaks arise from molecules desorbed from the surface rather than from ionization and subsequent fragmentation (dissociative photoionization) of higher mass molecules, thus supporting our assumption that fatty acids are the most likely assignment.

On the basis of the measured IEs, mass peaks between m/z = 290–500 are most likely lignin dimers, trimers, and their fragments. In Sollins' work,[18] alkaline cupric-oxide (CuO) oxidation

was used to quantify lignin, and the degradation products of vanilly-based, syringyl-based and cinnamyl-based lignin were also detected. However, with this method, the original oligomer structure was destroyed and no molecular information of the lignin compounds could be inferred. Based on their observed degradation lignin product and the mass peaks observed in our mass spectra, the 8-5 linkage type in guaiacyl-syringyl (G-S) lignin dimer and the 8-O-4 linkage type lignin trimer are postulated, and the possible molecular structures are shown in Figure 2. Notice that in our method, the precise isomer cannot be identified, hence the G-G-G lignin trimer could be a G-S-H (guaiacyl-syringyl-p-hydroxyphenyl) or H-S-G lignin trimer if one of the $–OCH_3$ group moves from one aromatic ring to another aromatic ring (figure 2). In the fragment mass region below m/z = 200, the fragment ions from guaiacyl (m/z = 137, $C_8H_9O_2^+$) and syringyl (m/z = 167, $C_9H_{11}O_3^+$) were observed.

In the previous study, Sollins (2009) reported an increase in the "microbial signature" of the organic matter in the denser fractions, and a corresponding decrease in the plant signature. Those results were based on the analyses of the stable isotope (^{13}C and ^{15}N), C/N ratio, the degree of oxidation of the lignin phenols and the substituted fatty acids (SFA) / lignin ratio. Here, we will show that the trend of an increasing microbial signature can also be observed in synchrotron-LDPI-MS. Figure 3a–g show mass spectra acquired for different density fraction samples at 10.5 eV. The lignin signals appeared in the lightest density fraction between m/z = 290–500 with their signal intensity decreasing with increasing density of the respective physical fraction. In contrast, the mass spectra of the denser fractions (figure 3 c–g) are composed of a series of fragments with a regular mass interval. Figure 4 shows the comparison mass spectra between the lightest (< 1.6 g cm^{-3}) and densest (> 3.0 g cm^{-3}) soil fraction at 9 eV and 11 eV.

At 9 eV the fragment signals below 200 Da are dominant in the fraction > 3.0 g cm^{-3}, in contrast to the fraction < 1.6 g cm^{-3}, which shows discrete signal peaks between mass-to-charge ratio (m/z) of 200–500. As the ionization energy is increased to 11 eV, more fragment peaks appear with a mass interval of 14 Da (loss of CH_2 group) between m/z 40–300 in the fraction > 3.0 g cm^{-3} (figure 4b). This suggests that there are long chain un-branched aliphatic hydrocarbons which could be derived from microbial-like fatty acids. Consequently, in our synchrotron-LDPI-MS obtained from different density fractions, the SOM change from being plant-like (lignins or plant lipids) to microbial-like (long chain aliphatic hydrocarbons) can be clearly observed. Notice that these characteristic lignin signals and a series of fragments with a 14 Da spacing (loss of a CH_2 group) are also observed in the mass spectrum of the bulk sample, as shown in figure 3a. The relative lignin concentration at different densities were estimated by integrating the mass peak area of the lignin signals (m/z = 484, 412, 396, 379, 353, 299). The integrated signal of lignin as a function of fraction density is compared to the data of Sollins *et al*. in Figure 5a. The two curves are normalized based on signal intensity in the light density fraction for visual clarity. The result shows that the lignin contribution decreased as the density increased and the general trend is in good agreement with the values reported by Sollins *et al* (2009). Notice that Sollins *et al*. used a chemical degradation method to quantify lignin monomers and fatty acids from cutin and suberin, and it is possible that this method is only sensitive to certain subsets of lignin and fatty acids. Synchrotron-LDPI-MS most likely encompasses a more complete representation of the organics in the system, however, it is difficult to assign every mass peaks in mass spectra obtained from a complex system like soil, and the concentration of lignin could be underestimated in our synchrotron-LDPI-MS, all of

these effects could account for the differences between our data and those reported by Sollins' *et al.*

In addition to organic matter, observing the mineral composition is important because contact with mineral surfaces is increasingly recognized as a critical control on soil carbon turnover.[24] Compared to organic compounds, the mineral material is less volatile and needs higher laser powers to either desorb or ablate from the sample surface. Again, too high a laser power will thermally decompose organic molecules, and it will be difficult to deconvolute mineral mass peaks from the overlapping complex organic fragment patterns. To avoid this problem, we used the ability of SIMS to release inorganic compounds of interest from the sample surface as demonstrated in previous work.[25] In positive SIMS, based on the SIMS spectra library provide from IONTOF (the vendor of the experimental apparatus), Fe^+, FeH^+, Si^+ and $SiHO^+$ ions are observed. The contributions of these secondary ions from different density fractions are shown in Figures 5b–c and compared to Sollins' data obtained from oxalate extractions of metals from soil samples.

SIMS signals are very sensitive to sample topography and matrix effects makes quantification difficult, but the general trends observed in SIMS are in good agreement with the literature, especially for Si^+ and $SiHO^+$, where both ion signals have a very similar trend between the density of 2.65 g cm^{-3} and 3.0 g cm^{-3}. All data obtained from synchrotron-LDPI-MS (lignin and fatty acid) and SIMS (mineral) are consistent with the data reported in Sollins *et al*. (2009), which support a general pattern of an increase in extent of microbial processing with increasing organo-mineral particle density.[26] However, unlike the previous study, both SOM and mineral compounds were observed directly from the sample surface, and not with a chemical extraction method, hence allowing us to trace both SOM and mineral compounds on the same surface. We

point out that by rastering the sample stage, it would even be possible to obtain location specific information (i.e., imaging mass spectroscopy) to test hypotheses regarding the site dependency of interactions between organic and mineral phases.

CONCLUSION

We applied synchrotron-LDPI-MS and SIMS to fractionated soil samples to observe organic and mineral compounds, respectively. Our results show that synchrotron-LDPI-MS provides a fast (~10 second for each measurement) and sensitive detection of organics in soil (only ~5 mg of each sample is needed in this study). Tuning the synchrotron photon energy and UV laser power allowed us to control the fragmentation and therefore identify chemical compounds with less ambiguity. The photoionization efficiency measurements provide useful information to distinguish different classes of organic matters. The wide variable range of UV laser power also allows us to selectively desorb molecules at low laser power to preserve molecular integrity. The contribution of both lignin and mineral compounds at different density fraction soil were estimated and compared to literature values. Although there are quantitative differences between our data and the literature, the general qualitative trends in the comparison of different density are very similar. While the ultimate goal is to directly image the chemical composition of a soil ecosystem, the density fraction experiments in this study provide useful information (a mass spectral library) and a calibration of the different chemical components and their signatures with VUV photoionization. The methods described here are also being used to quantify organic composition and structure of melanin polymers in bird feathers, perform single cell imaging mass spectrometry on plant biomass, and follow chemical change in bacteria-antibiotic

interactions. Hence synchrotron-LDPI-MS in combination with SIMS promises to be a unique tool to investigate molecular properties in a variety of environments.

ACKNOWLEDGEMENT

This work is supported by the Director, Office of Science, Office of Basic Energy Sciences, and by the Division of Chemical Sciences, Geosciences, and Biosciences of the U.S. Department of Energy at LBNL under Contract No. DE-AC02-05CH11231.

SUPPORTING INFORMATION

The following figures are available as supporting information.

Figure S1 shows the photoionization efficiency (PIE) curves for mass peaks observed in the lightest density faction (1.6 g cm^{-3}) of Susua soil.

Figure S2 shows synchrotron-LDPI-MS of the lightest fraction (1.6 g cm^{-3}) of Susua soil at 10.5 eV with various UV laser powers.

FIGURE CAPTIONS

Figure 1. Synchrotron-LDPI-MS of the lightest fraction (1.6 g cm^{-3}) of Susua soil at VUV photon energy of (a) 9 eV, (b) 11 eV, and (c) 14 eV with UV desorption laser energy of 3.7 MW cm^{-2}.

Figure 2. Proposed structures for lignin molecules observed in the lightest fraction (1.6 g cm^{-3}) of Susua soil.

Figure 3. Synchrotron-LDPI mass spectra taken with 38 laser pulses / 30 μm-diameter spot at 10.5 eV of Susau soil of (a) bulk sample, and at different densities of (b) 1.6 g cm^{-3}, (c) 2.15 g cm^{-3}, (d) 2.45 g cm^{-3}, (e) 2.65 g cm^{-3}, (f) 2.80 g cm^{-3}, and (g) 3.00 g cm^{-3}.

Figure 4. Comparison of Susua soil synchrotron-LDPI mass spectra obtained from the lowest density (LD) of 1.6 g cm^{-3}, and the highest density (HD) of 3.0 g cm^{-3} at photon energy of (a) 9 eV and (b) 11 eV. (c) The expanded view of (b) in the mass range between m/z= 120 to m/z = 360.

Figure 5. Distribution of (a) lignin obtained from synchrotron-LDPI (green solid square), and mineral material of (b) Fe^+ (green solid square) / FeH^+ (blue open circle), and (c) Si^+ (green solid square)/ $SiHO^+$ (blue open circle) obtained from positive ion SIMS across the density fractions. The total lignin signal obtained from synchrotron-LDPI; the total mineral signal derived from positive ion SIMS. The signal intensities are normalized with respect to each other. Data from Sollins *et al.*[18] are shown as red open triangles.

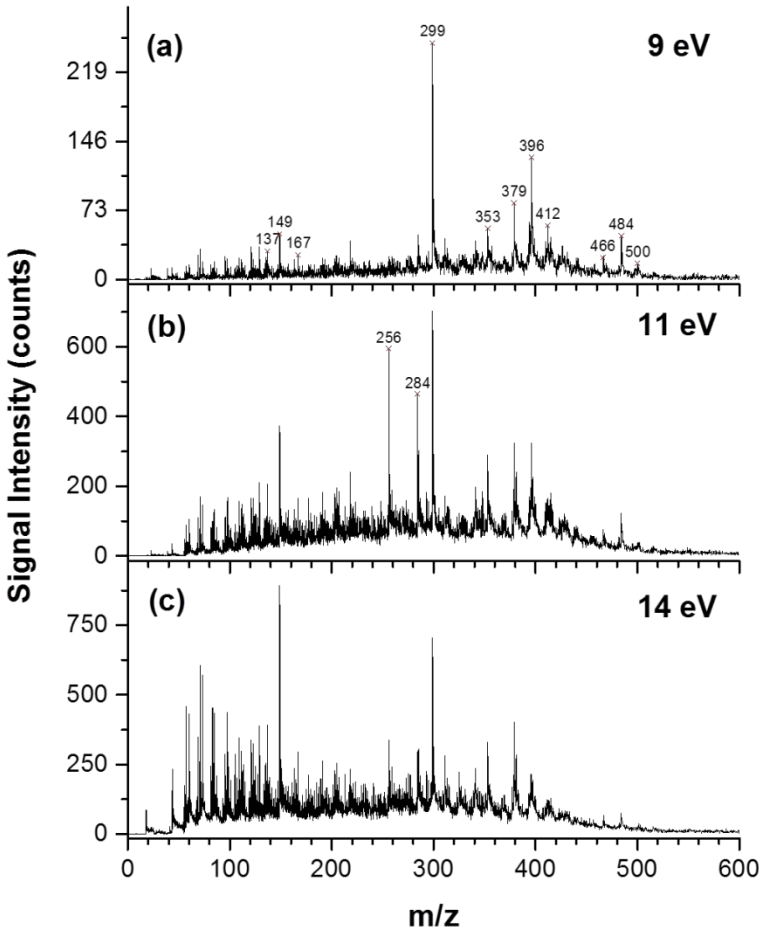

Figure 1. Synchrotron-LDPI-MS of the lightest fraction (1.6 g cm^{-3}) of Susua soil at VUV photon energy of (a) 9 eV, (b) 11 eV, and (c) 14 eV with UV desorption laser energy of 3.7 MW cm^{-2}.

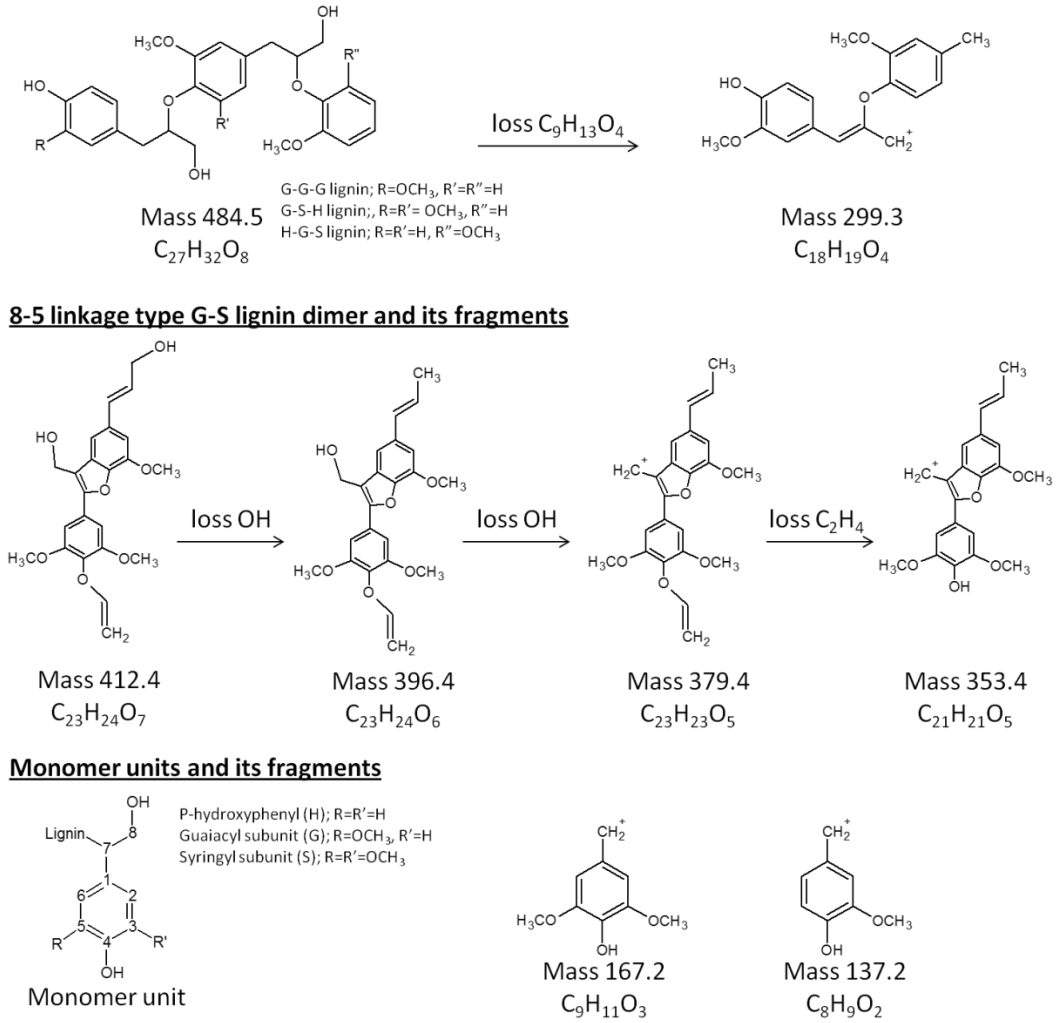

Figure 2. Proposed structures for lignin molecules observed in the lightest fraction (1.6 g cm^{-3}) of Susua soil.

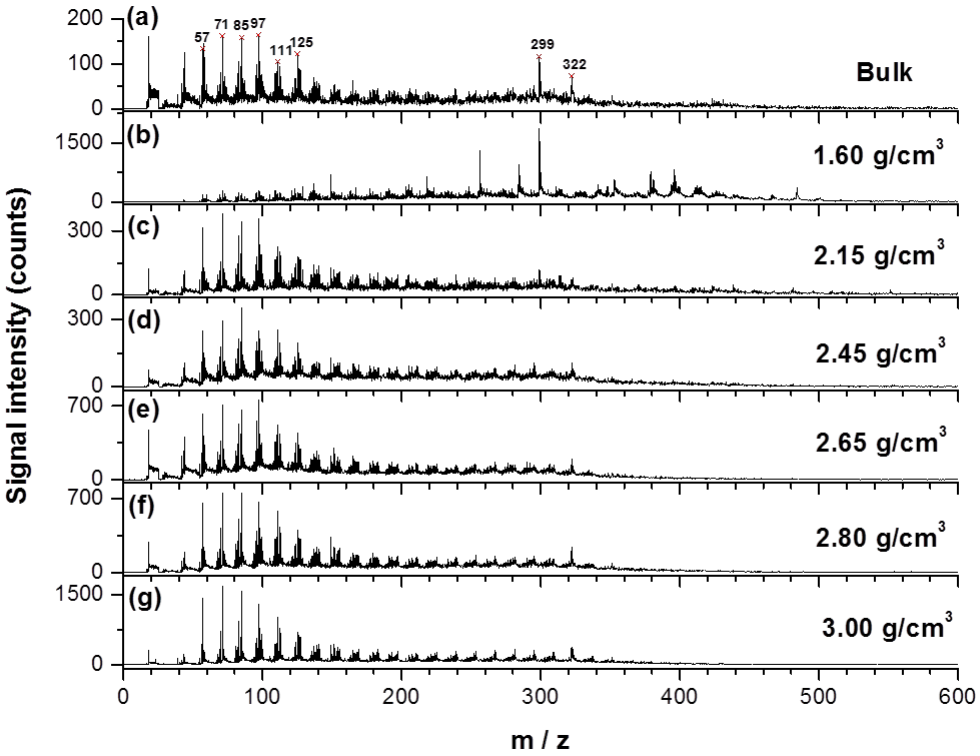

Figure 3. Synchrotron-LDPI mass spectra taken with 38 laser pulses / 30 μm-diameter spot at 10.5 eV of Susau soil of (a) bulk sample, and at different densities of (b) 1.6 g cm^{-3}, (c) 2.15 g cm^{-3}, (d) 2.45 g cm^{-3}, (e) 2.65 g cm^{-3}, (f) 2.80 g cm^{-3}, and (g) 3.00 g cm^{-3}.

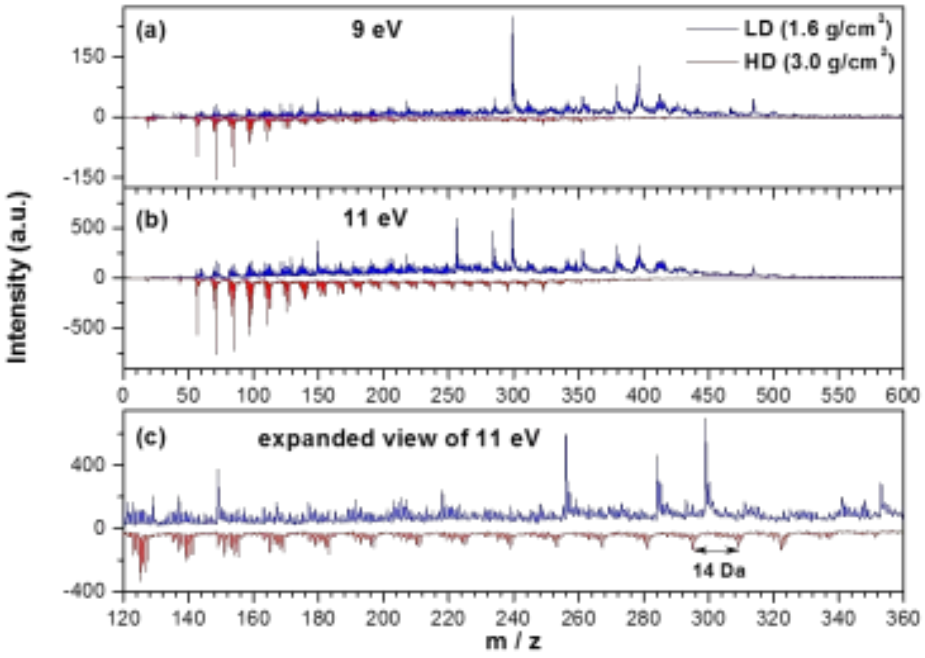

Figure 4. Comparison of Susua soil synchrotron-LDPI mass spectra obtained from the lowest density (LD) of 1.6 g cm^{-3}, and the highest density (HD) of 3.0 g cm^{-3} at photon energy of (a) 9 eV and (b) 11 eV. (c) The expanded view of (b) in the mass range between m/z= 120 to m/z = 360.

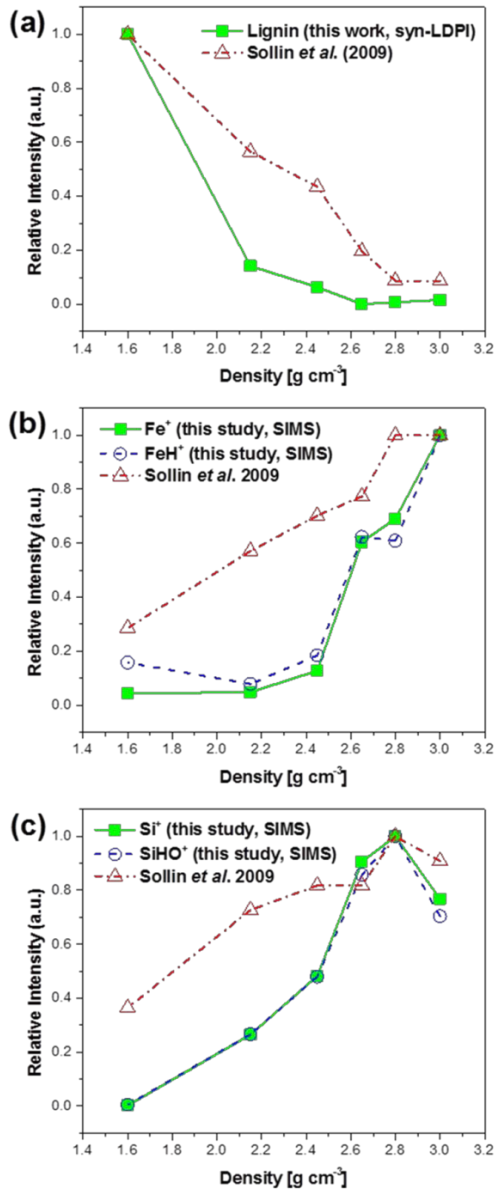

Figure 5. Distribution of (a) lignin obtained from synchrotron-LDPI (green solid square), and mineral material of (b) Fe^+ (green solid square) / FeH^+ (blue open circle), and (c) Si^+ (green solid square)/ $SiHO^+$ (blue open circle) obtained from positive ion SIMS across the density fractions. The total lignin signal obtained from synchrotron-LDPI; the total mineral signal derived from positive ion SIMS. The signal intensities are normalized with respect to each other. Data from Sollins *et al.*[18] are shown as red open triangles.

REFERENCES

(1) (a) Schmidt, M. W. I.; Knicker, H.; Hatcher, P. G.; KogelKnabner, I. *Eur. J. Soil Sci.* **1997,** *48*, 319-328; (b) Gelinas, Y.; Baldock, J. A.; Hedges, J. I. *Org. Geochem.* **2001,** *32*, 677-693; (c) Kogel-Knabner, I. *Geoderma.* **1997,** *80*, 243-270.

(2) Kleber, M.; Johnson, M. G. *Adv. Agron.* **2010,** *106*, 77-142.

(3) (a) Torn, M. S.; Trumbore, S. E.; Chadwick, O. A.; Vitousek, P. M.; Hendricks, D. M. *Nature* **1997,** *389*, 170-173; (b) Kaiser, K.; Guggenberger, G. *Eur. J. Soil Sci.* **2003,** *54*, 219-236; (c) Keiluweit, M.; Bougoure, J. J.; Zeglin, L. H.; Myrold, D. D.; Weber, P. K.; Pett-Ridge, J.; Kleber, M.; Nico, P. S. *Geochim. Cosmochim. Acta* **2012,** *95*, 213-226.

(4) (a) Meuzelaar, H. L. C.; Windig, W.; Harper, A. M.; Huff, S. M.; Mcclennen, W. H.; Richards, J. M. *Science* **1984,** *226*, 268-274; (b) Schulten, H. R.; Simmleit, N.; Mueller, R. *Anal. Chem.* **1987,** *5*, 2903-2908.

(5) (a) Leinweber, P.; Schulten, H.-R. *J. Anal. Appl. Pyrol.* **1995,** *32*, 91-110; (b) Leinweber, P.; Schulten, H.-R. *J. Anal. Appl. Pyrol.* **1999,** *47*, 165-189.

(6) Sobeih, K. L.; Baron, M.; Gonzalez-Rodriguez, J. *J. Chromatogr. A* **2008,** *1186*, 51-66.

(7) Campo, J.; Nierop, K. G. J.; Cammeraat, E.; Andreu, V.; Rubio, J. L. *J. Chromatogr. A* **2011,** *1218*, 4817-4827.

(8) Haider, K.; Schulten, H. R. *J. Anal. Appl. Pyrol.* **1985,** *8*, 317-331.

(9) Schnitzer, M.; Schulten, H. R. *Soil Sci. Soc. Am. J.* **1992,** *56*, 1811-1817.

(10) Neff, J. C.; Townsend, A. R.; Gleixner, G.; Lehman, S. J.; Turnbull, J.; Bowman, W. D. *Nature* **2002,** *419*, 915-917.

(11) Schulten, H.-R.; Leinweber, P. *J. Anal. Appl. Pyrol.* **1996,** *38*, 1-53.

(12) Saiz-Jimenez, C. *Environ. Sci. Technol.* **1994,** *28*, 1773-1780.

(13) Kostko, O.; Takahashi, L. K.; Ahmed, M. *Chem-Asian J.* **2011,** *6*, 3066-3076.

(14) Wilson, K. R.; Jimenez-Cruz, M.; Nicolas, C.; Belau, L.; Leone, S. R.; Ahmed, M. *J. Phys. Chem. A* **2006,** *110*, 2106-2113.

(15) Isaacman, G.; Wilson, K. R.; Chan, A. W. H.; Worton, D. R.; Kimmel, J. R.; Nah, T.; Hohaus, T.; Gonin, M.; Kroll, J. H.; Worsnop, D. R.; Goldstein, A. H. *Anal. Chem.* **2012,** *84*, 2335-2342.

(16) Eschner, M. S.; Selmani, I.; Groger, T. M.; Zimmermann, R. *Anal. Chem.* **2011,** *83*, 6619-6627.

(17) Hanley, L.; Zimmermann, R. *Anal. Chem.* **2009,** *81*, 4174-4182.

(18) Sollins, P.; Kramer, M. G.; Swanston, C.; Lajtha, K.; Filley, T.; Aufdenkampe, A. K.; Wagai, R.; Bowden, R. D. *Biogeochemistry* **2009,** *96*, 209-231.

(19) Moni, C.; Derrien, D.; Hatton, P. J.; Zeller, B.; Kleber, M. *Biogeosciences* **2012,** *9*, 5181-5197.

(20) Hedges, J. I.; Mann, D. C. *Geochim. Cosmochim. Ac.* **1979,** *43*, 1803-1807.

(21) Goni, M. A.; Hedges, J. I. *Geochim. Cosmochim. Ac.* **1990,** *54*, 3073-3081.

(22) Takahashi, L. K.; Zhou, J.; Kostko, O.; Golan, A.; Leone, S. R.; Ahmed, M. *J. Phys. Chem. A* **2011,** *115*, 3279-3290.

(23) Mysak, E. R.; Wilson, K. R.; Jimenez-Cruz, M.; Ahmed, M.; Baer, T. *Anal. Chem.* **2005,** *77*, 5953-5960.

(24) Conant, R. T.; Ryan, M. G.; Agren, G. I.; Birge, H. E.; Davidson, E. A.; Eliasson, P. E.; Evans, S. E.; Frey, S. D.; Giardina, C. P.; Hopkins, F. M.; Hyvonen, R.; Kirschbaum, M. U. F.; Lavallee, J. M.; Leifeld, J.; Parton, W. J.; Steinweg, J. M.; Wallenstein, M. D.; Wetterstedt, J. A. M.; Bradford, M. A. *Glob. Change Biol.* **2011,** *17*, 3392-3404.

(25) Takahashi, L. K.; Zhou, J.; Wilson, K. R.; Leone, S. R.; Ahmed, M. *J. Phys. Chem. A* **2009,** *113*, 4035-4044.

(26) Sollins, P.; Swanston, C.; Kleber, M.; Filley, T.; Kramer, M.; Crow, S.; Caldwell, B. A.; Lajtha, K.; Bowden, R. *Soil Biol. Biochem.* **2006,** *38*, 3313-3324.

FOR TOC ONLY

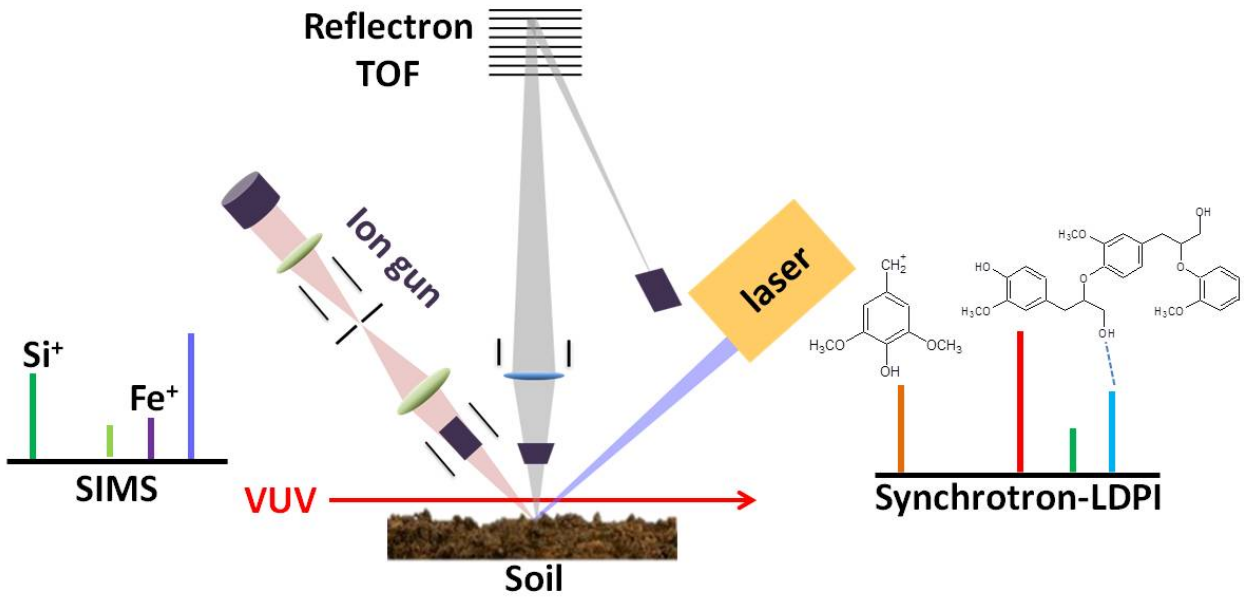
Reflectron
TOF
Ion gun
laser
Si+
Fe+
SIMS
VUV
Soil
Synchrotron-LDPI

Synchrotron based mass spectrometry to investigate the molecular properties of mineral-organic associations

Suet Yi Liu,[1] Markus Kleber,[2] Lynelle K. Takahashi,[1] Peter Nico,[3] Marco Keiluweit,[2,4] Musahid Ahmed[1,]*

[1] Chemical Science Division, Lawrence Berkeley National Laboratory, Berkeley, CA, USA

[2] Department of Crop and Soil Science, Oregon State University, Corvallis, OR, USA

[3] Earth Sciences Division, Lawrence Berkeley National Laboratory, Berkeley, CA, USA

[4] Chemical Sciences Division, Lawrence Livermore National Laboratory, Livermore, CA, USA.

* Corresponding author, mahmed@lbl.gov

SUPPLEMENTARY INFORMATION

Figure S1 shows the photoionization efficiency (PIE) curves for mass peaks observed in the lightest density faction (1.6 g cm^{-3}) of Susua soil. The photon energy was scanned between 7.4 and 12.0 eV, and mass spectra were collected at 0.1 eV photon energy intervals. Areas under the parent and fragment ion peaks were integrated at each photon energy, and the area plotted as a function of photon energy. A gas filter and MgF_2 window combination was used to remove higher order harmonics produced by the synchrotron. . As shown, the measured ionization energies (IEs) for mass peak at m/z = 484, 396, 379, 341, 299 are around 7.7 eV, and the measured IEs for mass peaks at m/z = 284, 256 are around 8.4 eV.

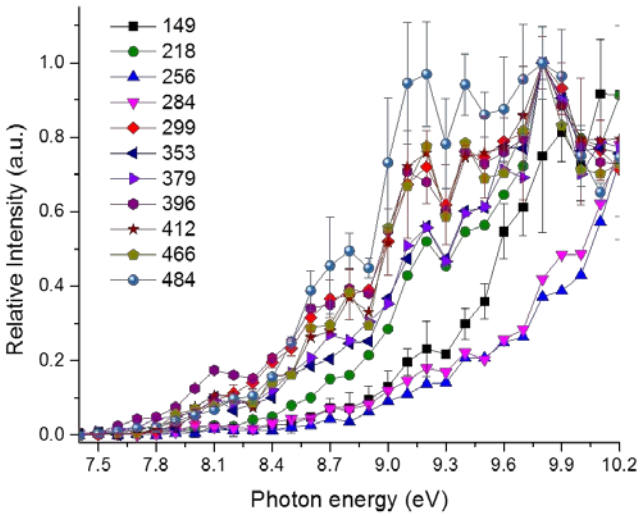

Figure S1. Synchrotron-LDPI PIE of mass peaks observed in the lightest fraction (1.6 g cm^{-3}) of Susua soil. The error bars of m/z = 149, 299 and 484 are shown to represent the errors of three different peak intensities.

Figure S2 shows synchrotron-LDPI-MS of the lightest fraction (1.6 g cm^{-3}) of Susua soil at 10.5 eV with various UV laser powers. Below the laser power of 0.7 MW cm^{-2}, no ion was observed, and ion signals started to appear at 1.5 MW cm^{-2}. As the laser power increases to 6.3 MW cm^{-2}, the fragment below m/z = 200 become more prominent, which arises from thermal dissociation from excess laser power. Compared to high mass range at m/z = 299 and above, mass peaks at m/z = 256 and 284 appear at lower laser power, suggesting that these two mass peaks are attributed to more volatile compounds, and therefore belongs to different classes of organic molecules.

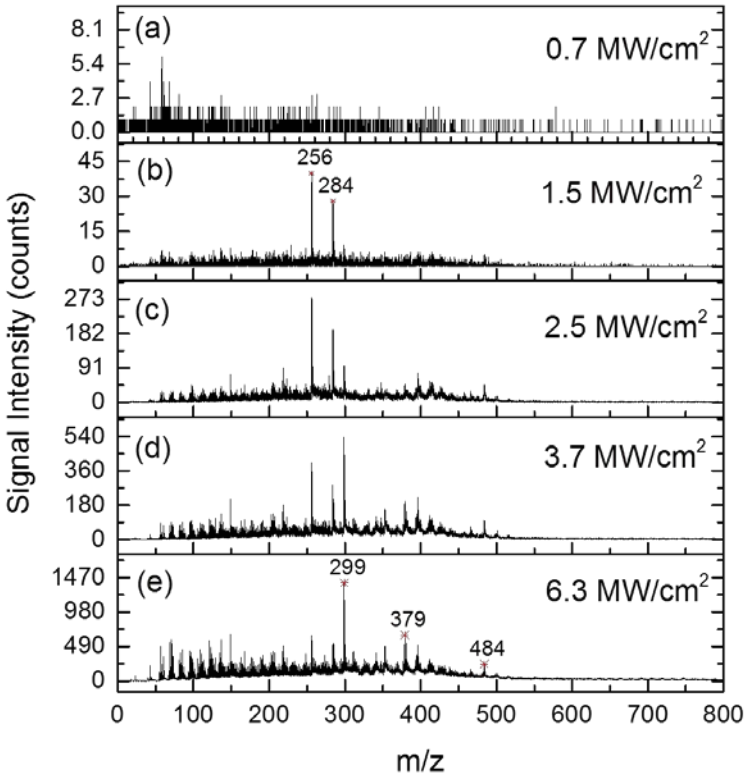

Figure S2. Synchrotron-LDPI -MS of the lightest fraction (1.6 g cm^{-3}) of Susua soil at VUV photon energy of 10.5 eV with UV desorption laser power of (a) 0.7 MW cm^{-2}, (b) 1.5 MW cm^{-2}, (c) 2.5 MW cm^{-2}, (d) 3.7 MW cm^{-2}, and (e) 6.3 MW cm^{-2}.